

Article

Application of Thermal Labyrinth System to Reduce Heating and Cooling Energy Consumption

Minyeop Rim ^{1,2}, Uk-Joo Sung ¹ and Taeyeon Kim ^{2,*}

¹ Center for Climatic Environment Real-scale Testing, Korea Conformity Laboratories, 5 Jeongtong-ro, Deoksan-myeon, Jincheon-gun, Chungbuk 27873, Korea; minyeop@kcl.re.kr (M.R.); suj21c@kcl.re.kr (U.-J.S.)

² Department of Architectural Engineering, Yonsei University, 50 Yonsei-ro, Seodaemun-gu, Seoul 03722, Korea

* Correspondence: tkim@yonsei.ac.kr (T.K.); Tel.: +82-02-2123-5783

Received: 9 August 2018; Accepted: 10 October 2018; Published: 15 October 2018



Abstract: To reduce the energy consumption in buildings, modern buildings are increasingly becoming airtight. In these structures, the outdoor air is supplied inside through mechanical ventilation systems, which are essential for ensuring comfortable indoor air quality. However, these systems consume a considerable amount of energy in buildings. One potential solution is using a thermal labyrinth system, which is buried underneath the building. It can pre-cool or pre-heat the outdoor air through heat transfer with the surrounding soil. In this research, a number of case studies were conducted to optimize the thermal labyrinth design. The optimized thermal labyrinth system was derived using computational fluid dynamics (CFD) simulation. In addition, operation algorithms were developed for the efficient operation of the thermal labyrinth system in buildings. The results indicated that there were five operation modes, and the thermal labyrinth could be operated for seven months of the year. The energy reduction effects of the thermal labyrinth system were analyzed and were assessed by the transient system simulation (TRNSYS) tool. A 12% reduction in the annual heating and cooling energy was achieved by applying the thermal labyrinth system.

Keywords: thermal labyrinth system; ventilation; energy consumption; heat transfer; passive; active; package

1. Introduction

1.1. Background

As an increasing number of air-tight buildings are being constructed in order to save energy, optimum ventilation systems that allow the outdoor air into a building have become essential [1]. When the outdoor air is used to operate the heating, ventilation, and air conditioning (HVAC) system, the cooling or heating energy consumption in the building would increase in order to adjust the air temperature to a set point. Therefore, to reduce the energy consumption, an energy-saving HVAC system is required.

Energy-saving HVAC systems that use ground heat are mainly divided into tube-style (earth tube, earth tunnel, and earth-air-heat exchanger (EAHE)) and thermal labyrinth systems. Various studies have been conducted on the tube-style systems and verified its energy-saving effect [1,2]. Further to their findings, research has focused on improving the EAHE heat transfer efficiency in terms of length and diameter of the tube type heat exchanger, mass flow rate, laying depth, and changes in soil [3–5]. Previous literature has indicated that the tube-style system could apply to various climate conditions such as Italy [6], Turkey [7] and Malaysia [8]. Moreover, Yu et al. [9], Ghosal et al. [10] and Bansal et al. [11] sought to maximize the system energy saving effect by combining

the EAHE with another passive system or an active system, such as a solar chimney, air conditioner or an evaporative cooler. Yang et al. [12] described that the use of tube-style ventilation must be considered alongside building characteristics and categories because it cannot be quantified in isolation from the building characteristics.

Song et al. [13] analyzed the cooling, heating, and dehumidification of the thermal labyrinth system by measuring the internal temperature and humidity. Using an air current analysis program, Sohn et al. [14] analyzed the heat transfer efficiency in the ground-heat-based thermal labyrinth system based on the increase in the heat transfer area according to the change in shape of the openings which introduce outdoor air in the system.

Various studies have focused on the simulation and assessment of the tube-type ground-heat-based systems (such as EAHE, Earth Tube, and Earth Tunnel); however, few have focused on the thermal labyrinth system. In addition, few studies have investigated the potential improvements to the heat transfer efficiency of the thermal labyrinth system and its effective mode of operation.

A thermal labyrinth system introduces the outdoor air into a building through a thermal labyrinth, which is a concrete structure installed underground, and uses the ground heat produced by heat transfer to ventilate the building. According to Song et al. [13] and Sohn et al. [14], the thermal labyrinth system is easier to maintain and offers better energy efficiency than the tube type systems, because it possesses a larger contact area between the thermal labyrinth system and the outdoor air. Moreover, the thermal labyrinth system does not require an additional space, because it is installed underneath buildings. Therefore, this system is more suitable for South Korea, given the limited land availability.

1.2. Objectives

The objectives of this study were as follows:

- (1) To produce a thermal labyrinth design that can offer maximum heat transfer using the limited underground space of a building based on various case studies.
- (2) To propose an operational algorithm based on the performance analysis of the optimized thermal labyrinth system.
- (3) To reduce the yearly heating and cooling energy consumption of buildings by using the optimized thermal labyrinth design plan and the operational algorithm.

2. Case Studies: Optimized Thermal Labyrinth System

2.1. Description of the Sample Building and the Used Thermal Labyrinth System

In this section, various thermal labyrinth system designs that ensured maximum heat transfer efficiency were derived through different case studies by optimizing the design of the 412.68 m² concrete underground space. Figure 1 shows a sample building and its thermal labyrinth. The thermal labyrinth system was located three meters under the building and was constructed with concrete walls. Table 1 shows the conditions of the studied building and the thermal labyrinth system used in the case study.

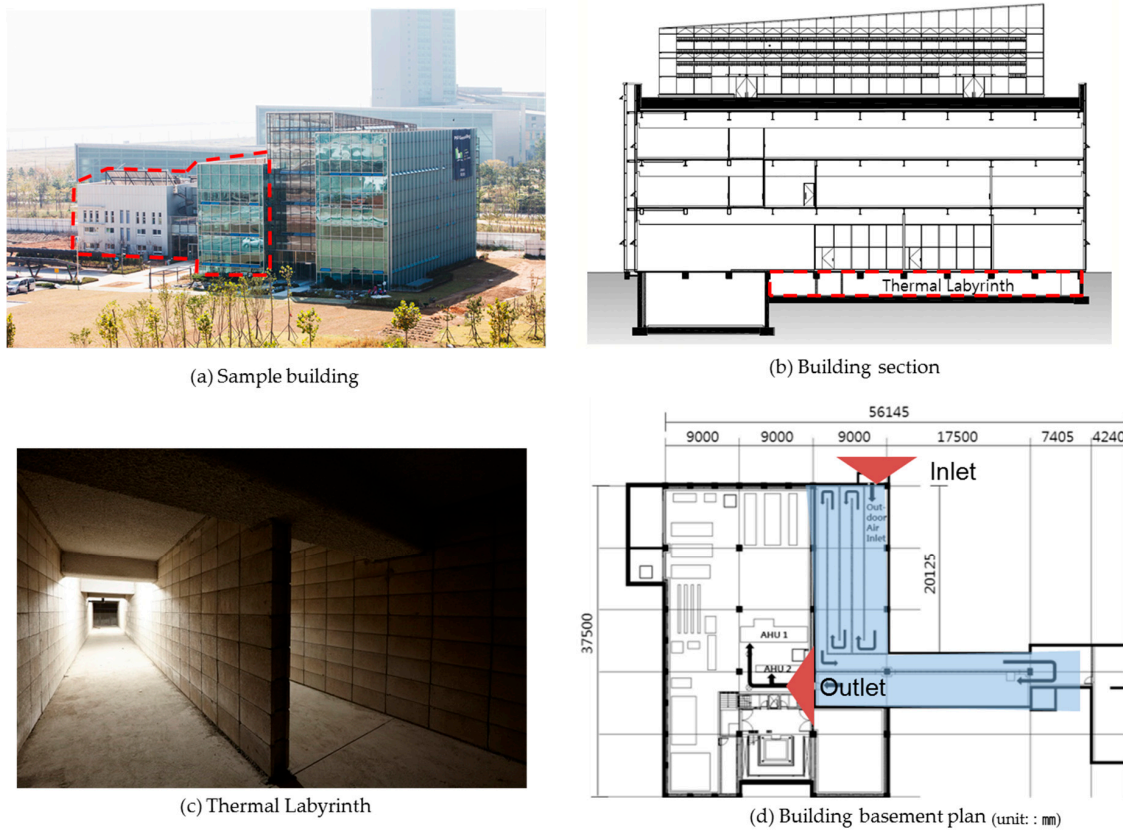


Figure 1. Photographs and plans of sample building. (a) Sample building; (b) Building Section; (c) Thermal Labyrinth; (d) Building basement plan.

Table 1. Conditions of the studied building and thermal labyrinth system.

General Information	Site	Incheon, South Korea
HVAC ** zone Information	Building type	Office
	System	AHU * with thermal labyrinth, radiant ceiling
	Area	605.55 m ²
	Ventilation requirement	7400 m ³ /h
	Minimum outdoor air requirement	2200 m ³ /h
Thermal labyrinth space conditions	Depth	3 m
	Area	412.68 m ²
	Material	Concrete
Fan information used with thermal labyrinth	Fan type	Air foil
	Air flow rate	2200 m ³ /h
	Efficiency	63%
	Fan static pressure	246.97 mmAq
	COP *** calculation	Quantity of heat/ shaft power

* AHU: Air handling unit ** HVAC: Heating, ventilation, and air conditioning *** COP: Coefficient of performance.

2.2. CFD Simulation for the Case Study

2.2.1. Modeling

Accurately depicting the thermal conduction through soil is important for simulating the thermal labyrinth system using computational fluid dynamics (CFD) simulation. A previous study simulated the thermal conduction by modeling the cooling tube with the surrounding earth when analyzing the ground-heat-based heat transfer system, using a fluid analysis program [14] to make the simulated results as close to the actual system as possible. In this case study, the thermal labyrinth system and underlying ground were also modeled together (Figure 2).

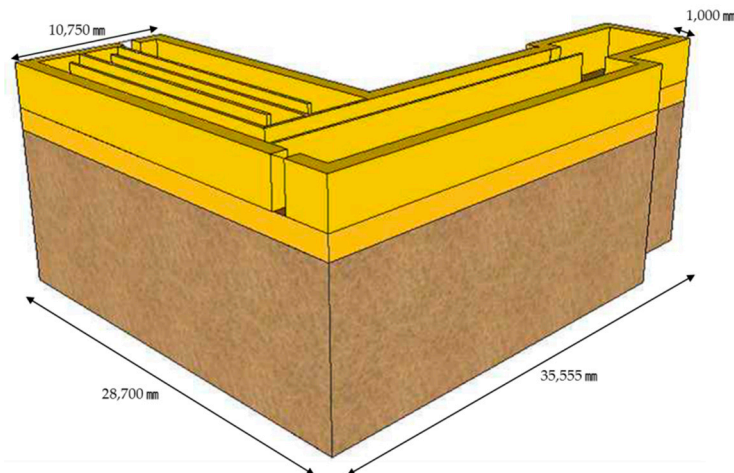


Figure 2. Earth modeling for thermal labyrinth analysis.

2.2.2. Case Conditions

According to the previous studies, the methods that can be used to increase the ground heat-based system efficiency are: Changes in the speed of the internal air current; changes in the soil conditions; and changes in the length, section area, and heat transfer surface. Since the air current speed used in the thermal labyrinth system in the target building is determined according to the amount of ventilated air required for the target HVAC space, the air current speed is considered a constant and cannot be changed. In addition, once the site of the target building is determined, the soil conditions can no longer be changed. Therefore, in this study, changes in the surface area of the internal thermal labyrinth system were used as the case's only variable condition (Table 2).

Table 2. Cases set considered for the simulation.

Variable	Case	Condition
1. Length variation	1-1	Short (126 m)
	1-2	Medium (162 m)
	1-3	Long (257 m)
2. Surface shape variation	2-1	No fin
	2-2	Fin on the wall
	2-3	Fin on the wall and floor (3000 mm gap)
	2-4	Fin on the wall and floor (1500 mm gap)

2.2.3. Boundary Conditions and Solver Control

The thermal labyrinth system reduces the heating and cooling loads through heat transfer with surrounding soil which maintains the temperature below a certain temperature throughout the year. Therefore, the soil temperature is very important in analyzing the effect of the pre-heating and pre-cooling of the thermal labyrinth system.

This temperature is affected by various factors in addition to climate, such as the amount of moisture in the soil, flow pattern of the ground water, or shaded areas [15]. Therefore, it is difficult to describe the ground temperature data based only on the regional time and the ground depth. The ground temperatures are more influenced by weather and have greater diurnal variation near the surface. The influence of diurnal variation generally disappears about 1 m underground, and the influence of weather fades at about 6–7 m underground. Therefore, while there are significant monthly temperature changes due to solar radiation and ambient air near the ground surface, the ground temperature tends to stay constant as the depth increases, and it can be assessed with a periodic function. In this study, it was assumed that the target soil had a constant heat dissipation ratio. Using the heat dissipation coefficient, based on the heat dissipation ratio and the average temperature of

the surface, the distribution of the ground temperature was calculated as a function of time, based on Equation (1) [16].

$$T_{z,t} = T_m - A_z \exp \left[-z \left(\frac{\pi}{365\alpha} \right)^{\frac{1}{2}} \right] \cos \frac{2\pi}{365} \left[t - t_0 - \frac{z}{2} \left(\frac{365}{\pi\alpha} \right)^{\frac{1}{2}} \right] \quad (1)$$

$T_{z,t}$: Ground temperature at depth z based on time t ($^{\circ}\text{C}$)

T_m : Yearly average surface temperature ($^{\circ}\text{C}$)

A_z : Amplitude of temperature fluctuation ($^{\circ}\text{C}$)

z : Ground depth (m)

α : Soil thermal diffusion coefficient (m^2/day)

t : Days per year (days)

t_0 : Start date (days)

The coefficients used in Equation (1) were the ground temperature coefficients in Incheon (Table 3) [17]. The results of the calculation of the ground temperature using Equation (1) showed that below about 15 m, the ground temperature was 14.2°C . Hence, the temperature of the lower part of the earth was set to be 14.2°C in the simulation model shown in Equation (1). The heat transfer into the thermal labyrinth side could be determined by inputting the earth's thermal conductivity into the simulation (Table 4). Figure 3 is the diagram of heat transfer between soil, concrete and air.

Table 3. Coefficients used in the calculation of the ground temperature distribution.

T_m	A_s	z	t_0	α
14.2°C	14.65°C	0–20 (m)	30	$0.076 \text{ (m}^2/\text{day)}$

Table 4. Properties of the material applied to the simulation.

Material	Thermal Conductivity	Specific Heat	Density
Soil	$1.3 \text{ W/m}\cdot\text{k}$	$800 \text{ J/kg}\cdot\text{K}$	1599 kg/m^3
Concrete	$0.93 \text{ W/m}\cdot\text{k}$	$653 \text{ J/kg}\cdot\text{K}$	2300 kg/m^3

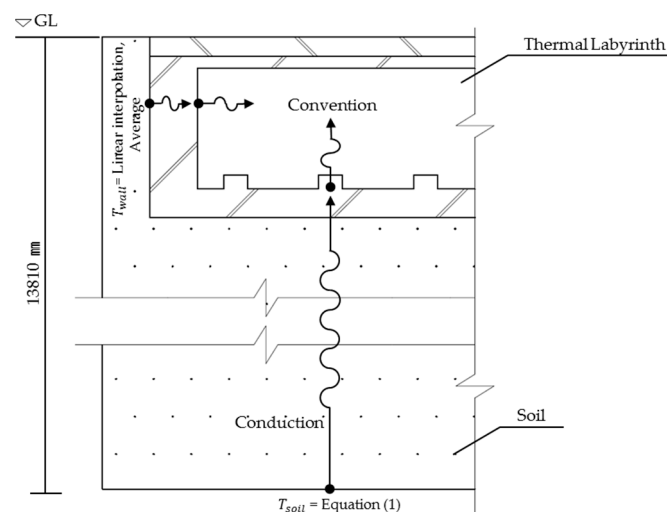


Figure 3. Heat transfer diagram.

The ceiling of the thermal labyrinth was adiabatic as it meets with the upper part of the structure. The part of the outer wall that touches the ground required additional arrangement as the ground temperature varied with depth. The present study estimated the temperature of this wall section

through linear interpolation and the basic trapezoid rule, and then uniformly applied the averaged value of the result to the wall section.

In Section 2, a CFD simulation software tool called star CCM+ was used to derive the optimal thermal labyrinth. It allows a detailed analysis of the ambient air passing through the thermal labyrinth and the thermal conductivity allows an accurate analysis of the heat transfer profile. For a more accurate analysis of the indoor thermal environment, the standard k- ϵ low-Reynolds-number model that allows an accurate analysis of heat transfer on the surface was applied. The low-Reynolds-number model can analyze the effect of viscosity on the surface more precisely by generating a uniform grid on the surface. Although it takes longer than the high-Reynolds-number model that makes rough calculations of the surface grid through the wall function at the surface level, it provides precision, making it suitable for assessing the thermal labyrinth system that mostly deals with heat transfer on the surface. The following are the detailed equations (Equations (2)–(7)) applied to the standard k- ϵ low-Reynolds-number model.

Continuity Equation:

$$\nabla \cdot \mathbf{V} = 0 \quad (2)$$

Equation of Motion:

$$\rho \frac{D\mathbf{V}}{Dt} = -\nabla p + \mu \nabla^2 \mathbf{V} + \rho \mathbf{f} \quad (3)$$

Energy Equation:

$$\frac{\partial}{\partial t}(\rho k) + \frac{\partial}{\partial x_j} \left[\rho k u_j - \left(\mu + \frac{\mu_t}{\sigma_k} \right) \frac{\partial k}{\partial x_j} \right] = P - \rho \epsilon - \rho D \quad (4)$$

Energy Dissipation Equation:

$$\frac{\partial}{\partial t}(\rho \epsilon) + \frac{\partial}{\partial x_j} \left[\rho \epsilon u_j - \left(\mu + \frac{\mu_t}{\sigma_\epsilon} \right) \frac{\partial \epsilon}{\partial x_j} \right] = (C_{\epsilon 1} f_1 P - C_{\epsilon 2} f_2 \rho \epsilon) \frac{\epsilon}{k} - \rho E \quad (5)$$

$$\mu_t = C_\mu f_\mu \rho \frac{k^2}{\epsilon} \quad (6)$$

$$P = \tau_{ij}^{turb} \frac{\partial u_i}{\partial x_j} \quad (7)$$

In the above equation, the applied values for each constant are shown in Table 5. The flow of the sublayer, which is affected by the viscosity of the wall surface, was analyzed by the low- y^+ model. The value of y^+ is set to <1 in the standard k- ϵ low-Reynolds-number model used in the present study. The total numbers of mesh elements are around 500,000–700,000 for the 7 studied cases. Detailed input conditions are shown in Table 6 and formed meshes are like Figure 4.

Table 5. Simulation constants.

D	1.0	E	0.00375
C_μ	0.09	$C_{\epsilon 1}$	1.44
$C_{\epsilon 2}$	1.92	σ_k	1.0
σ_ϵ	1.3	F_1	1.0
F_2	$1 - 0.3e - Re_t^2$		

Table 6. Simulation input conditions.

Item	Condition	
Mesh conditions	Mesh model	Polyhedral
	Base size	0.5
	Surface growth	1.3 (slow)
Physical conditions	Turbulence model	Standard k- ϵ low Reynolds number model
	Wall treatment	low- y^+ ($y \leq 1$)
	Convection scheme	Second S-order upwind scheme
	Inlet temperature	-2.4 °C
	Outlet velocity	0.34 m/s
	Soil temperature	14.2 °C
Air flow rate	2200 m ³ /h	

**Figure 4.** Scene with its mesh.

2.3. Results of the Case Studies

2.3.1. Assessment of the Heat Transfer Efficiency According to the Length of the Internal Thermal Labyrinth Area

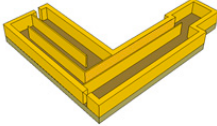
The results for the comparative analysis of the heat transfer effect according to different lengths of the internal thermal labyrinth area are summarized in Table 7, and divided into cases.

Figure 5 showed the pre-cooling and pre-heating effect of Case 1-2. The simulation results showed that as the length increased, the temperature difference between the inlet and outlet and the consequent amount of the heat acquired scarcely changed. However, the pressure difference showed a rapid increase (Figure 6).

This is because the increase in the length of the air current path inside the fixed space reduced the sectional area of the space where the air travelled.

As shown in Figure 7, there was a slight increase in the fan power due to the increase in the outlet pressure in the thermal labyrinth from Case 1-1 to Case 1-3. Accordingly, the coefficient of performance (COP) was shown to have been the highest in Case 1-1, where the pressure was the lowest. However, in all cases, the differences in the COP were similar; about 0.005. Thus, it was determined that there was no significant difference in the heat transfer effect unless the area that is connected to the ground changes drastically; in addition, if this area cannot be increased drastically, then it would be most efficient to minimize the increase in pressure.

Table 7. The studied cases for analyzing the impact of the change in the length on the heat transfer efficiency.

Case	Length (m)	Modeling
1-1	126	
1-2	162	
1-3	257	

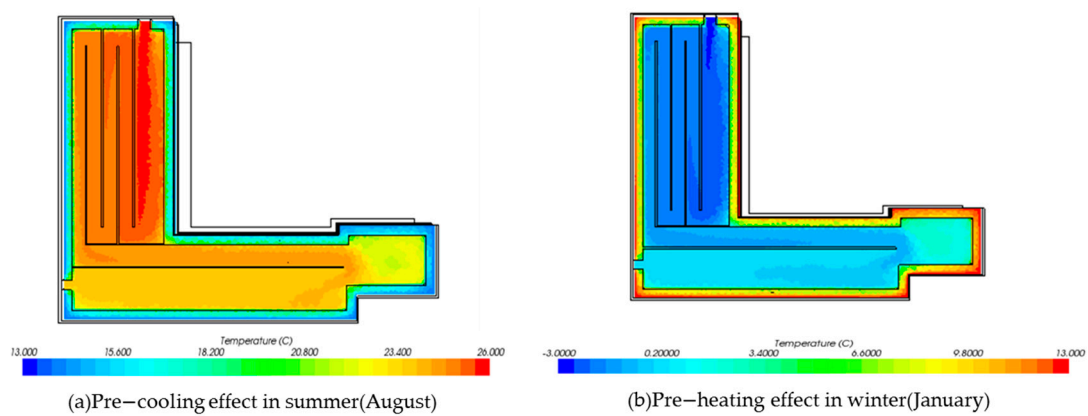


Figure 5. Example of pre-cooling and pre-heating effect (Case 1-2). (a) Pre-cooling effect in summer (August). (b) Pre-heating effect in winter (January).

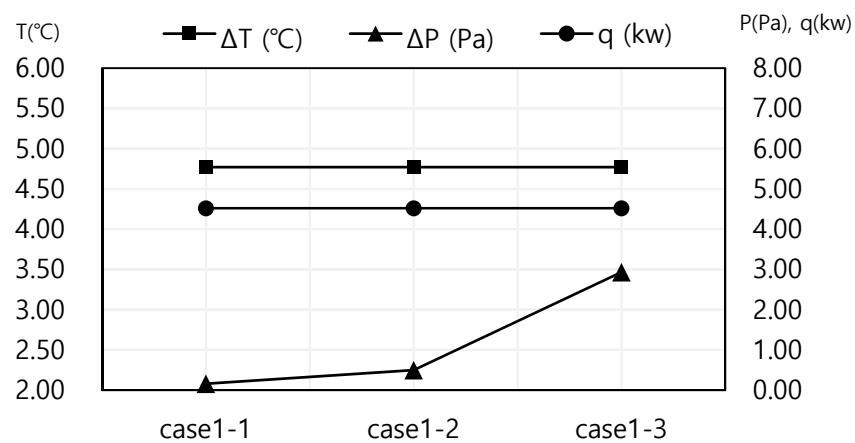


Figure 6. Change in temperature, pressure, and thermal capacity with length.

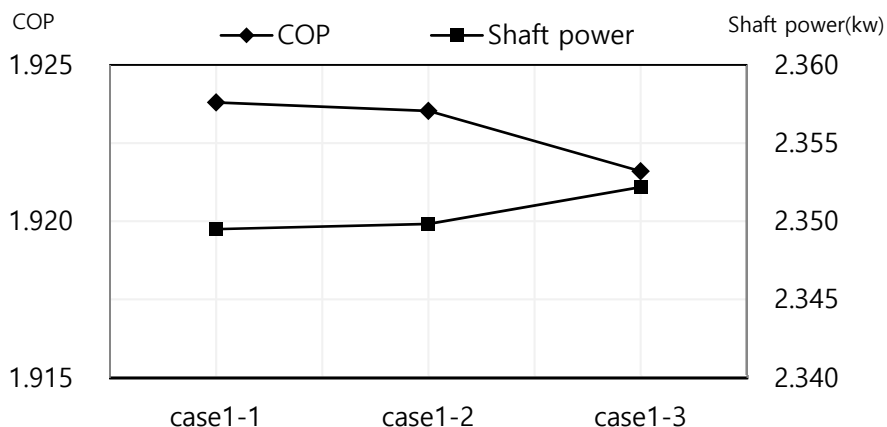


Figure 7. Air blower axial power and COP changes with length.

2.3.2. Assessment of the Heat Transfer Efficiency According to the Internal Shape

The comparative analysis of the heat transfer according to the change in the internal shape was categorized into cases as shown in Table 8. Owing to the internal embossed surfaces of the system, the heat transfer area between the air that passes through the interior and the ground may increase, and vortexes would be formed around these surfaces, which may result in enhanced heat delivery.

Table 8. The studied cases for analyzing the impact of the internal form change on the heat transfer efficiency.

Case	Shape Variation	Modeling
2-1	No fin	
2-2	Fin on the wall (300 mm depth)	
2-3	Fin on the wall and floor (300 mm depth, 3000 mm gap)	
2-4	Fin on the wall and floor (300 mm depth, 1500 mm gap)	

The simulation results showed that there were little changes in the temperature and the acquired heat between Case 2-1, which did not have any embossed surfaces, and Case 2-2, where there were embossed surfaces only on the walls (Figure 8). However, in Case 2-3, where there were embossed surfaces on the floor, the temperature change was relatively high, as was the subsequent heat acquired, and the pressure increased, so the overall COP was high (Figure 9). This shows that the heat transfer efficiency between the internal air and the floor improved due to the increase in the surface area of the floor. In Case 2-4, where the embossed surfaces were more tightly formed, the temperature difference between the inlet and the outlet was larger than in the other cases, thereby showing better heat transfer efficiency.

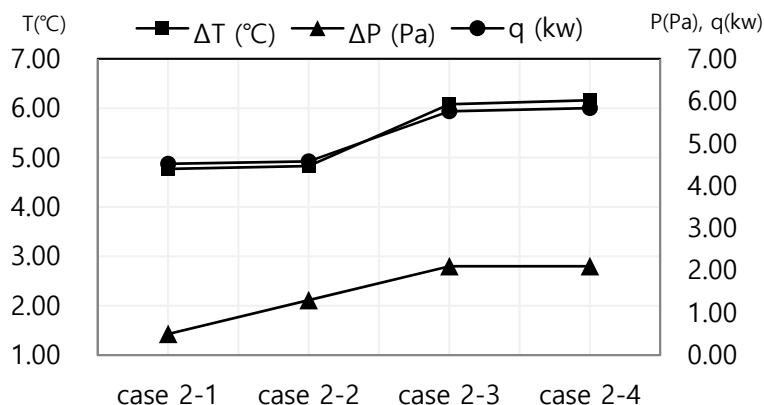


Figure 8. Changes in temperature, pressure, and thermal capacity with the internal form change.

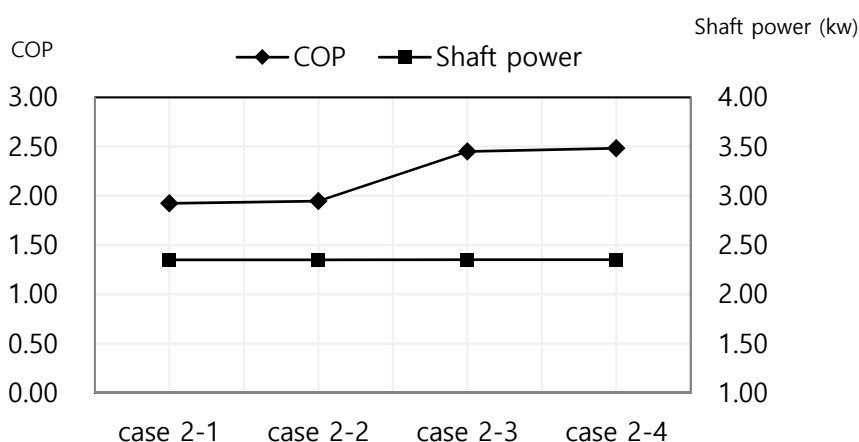


Figure 9. Changes in the axial power of the air blower and COP with the internal form change.

2.4. Analysis of the Performance of the Optimized Thermal Labyrinth

Based on the previous case studies, the design methods in the cases where the COP was high were integrated to derive an optimized thermal labyrinth that can produce maximum efficiency within the given underground space. Moreover, to determine the yearly heat transfer efficiency of the optimized thermal labyrinth, a CFD simulation was performed. The monthly average temperature was set to be the thermal labyrinth inlet temperature, and the other input conditions followed those used in the preceding case studies (Table 9).

The simulation results showed that in January, when the thermal labyrinth inlet temperature was the lowest, the inlet-outlet temperature difference was the largest at 6.17 °C, and the COP was 2.49. In August, when the thermal labyrinth inlet temperature was the highest, the inlet-outlet temperature difference was 3.78 °C, and the COP was 1.53. On the other hand, in April and October (transitional periods) the inlet-outlet temperature difference was small, so the COP dropped below 1.0 (Figure 10).

Based on the annual optimized thermal labyrinth performance data and using multiple regression analysis, the relationship between the outside air and the thermal labyrinth passage temperature is expressed as follows:

$$y = 0.0027x^2 + 0.5989x + 5.0246 \tag{8}$$

Table 9. The optimized conditions of the thermal labyrinth design.

Velocity (m/s)	Length (m)	Surface Shape
0.34	126	Fin on the wall and floor (500 mm gap)

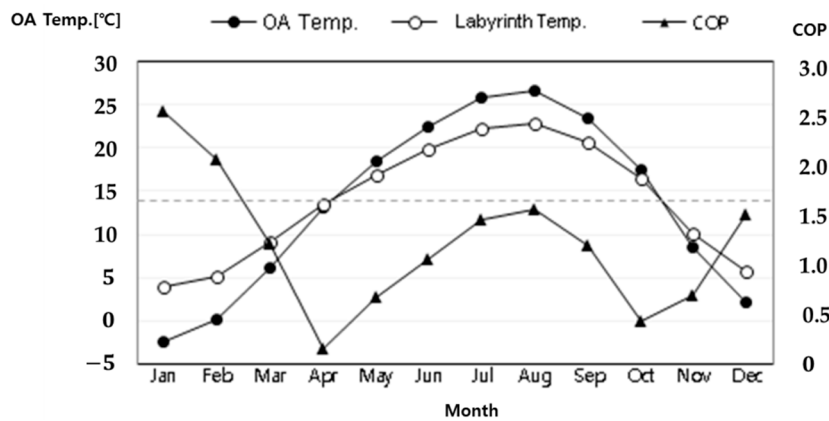


Figure 10. Monthly average outdoor air (OA) temperature, optimized thermal labyrinth temperature, and COP.

3. Operation Mode

In this section, the results of the performance analysis of the previously discussed optimal thermal labyrinth system were used to produce the optional mode of operation. The algorithm in Figure 11 was determined based on the internal temperature, outdoor air temperature, air temperature after the outdoor air passed through the thermal labyrinth, and ground temperature.

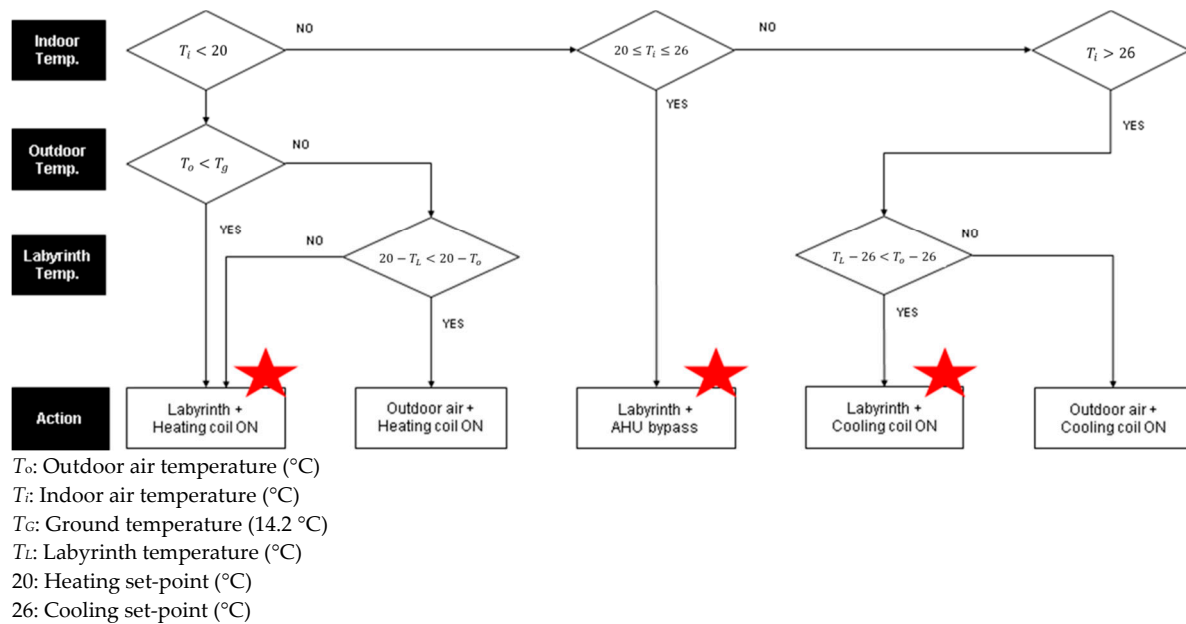


Figure 11. Thermal labyrinth system operational algorithm.

As shown in Figure 11, if the outdoor air temperature is lower than the ground temperature at 14.2 °C, then the temperature of the air after it passes through the thermal labyrinth would always be higher than the outdoor air temperature. However, if the outdoor air is higher than 14.2 °C, then the temperature of the air after it passes through the thermal labyrinth would be lower than the outdoor air temperature. Therefore, if the outdoor air temperature is lower than 14.2 °C during the heating season, the air that passes through the thermal labyrinth would be better used to heat the air handling unit (AHU) and to be supplied indoors. However, if the outdoor air temperature is higher than 14.2 °C, the outdoor air would be better used for air-conditioning. Moreover, when the indoor temperature is within the comfortable range of 20–26 °C, the outdoor air can be supplied indoors without heating or cooling. Therefore, the thermal labyrinth system can be used in three of the five operation modes.

4. Verification of the Heating and Cooling Energy Saving Effect of the Thermal Labyrinth System through TRNSYS Simulation

To determine the heating and cooling energy-saving effect when the proposed optimal thermal labyrinth system design and the operational algorithm are applied to the transient system (TRNSYS) energy simulation was performed. The yearly heating and cooling energy consumption with and without the installation of the optimized thermal labyrinth system operated according to the operational algorithm in the target building was compared.

4.1. System Description

Figure 12 shows sample building modeling and building description and Figure 13 shows the system chart of the target building. The HVAC system used for air-conditioning of the target zone contains the AHU, to which the thermal labyrinth system is connected, and the ceiling radiation air-conditioning system. This study was conducted to determine the heating and cooling energy-saving effect of the AHU with the use of the thermal labyrinth system, the TRNSYS model was set with the ceiling radiation air-conditioning system already operating. Table 10 shows input conditions for the simulation. Since none of the TRNSYS simulation components can realize the thermal labyrinth system, the temperature data after passing through it were created based on Equation (8), and were applied to the TRNSYS using the Type 9 Data Reader. Figure 14 shows TRNSYS modeling of the system with the building.

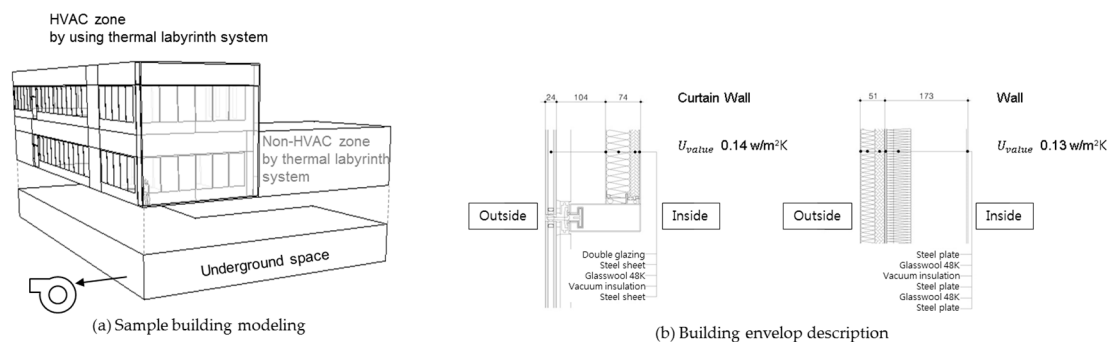


Figure 12. Sample building modeling and building envelop description.

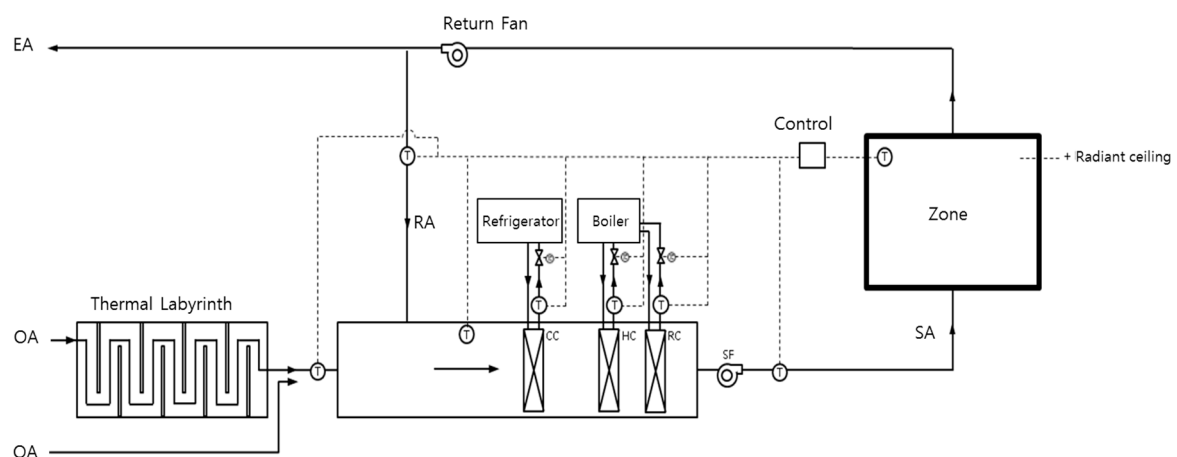
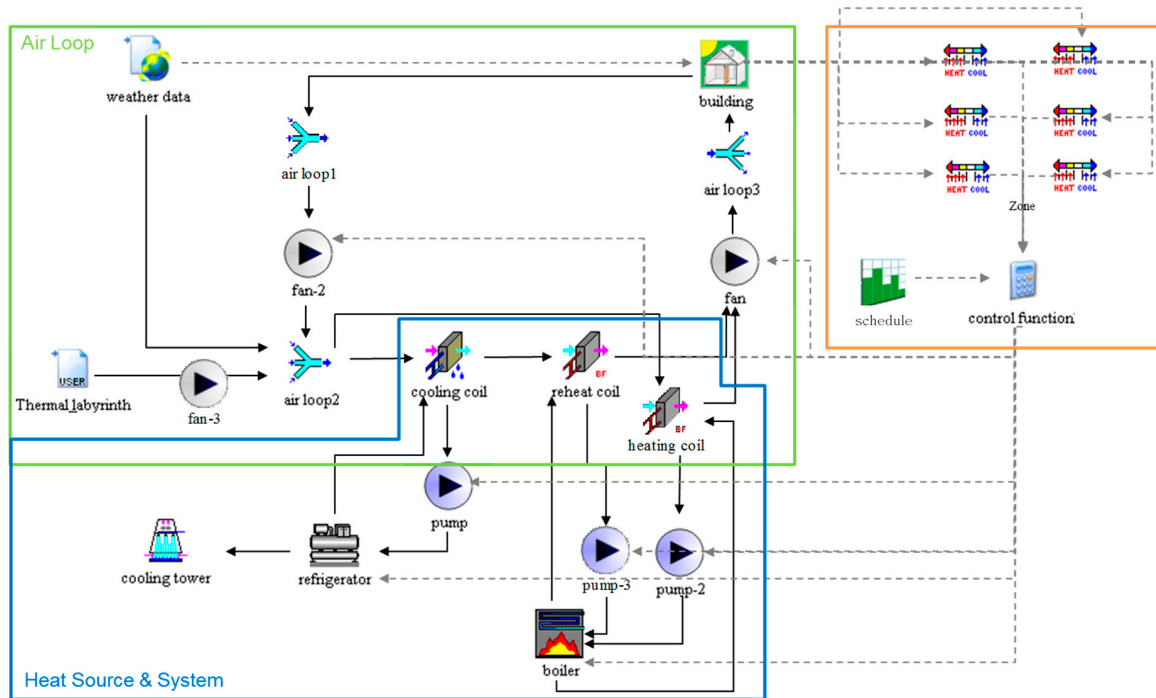


Figure 13. System construction in the studied building.

Table 10. Input conditions of TRNSYS simulation.

System	Single Duct CAV System	
Set point	Heating: 20 °C	Cooling: 26 °C
Schedule	09:00~18:00	
Ventilation	7400 m ³ /h	
Outdoor air	2200 m ³ /h	
Internal heat	Person: 0.2 W/m ² , Computer: 20 W/m ² Light: 10 W/m ²	

**Figure 14.** TRNSYS modeling of the system with the building.

4.2. Simulation Results

Figure 15 shows the indoor and outdoor air temperatures during heating in January. The indoor set temperature was 20 °C, and the indoor temperature during the working hours was set above 20 °C before and after the thermal labyrinth system was installed. The results showed that the heating system was working normally. It was operated only during the working hours according to the input schedule. The frequency of the heating system operation showed a difference between the two cases. Figure 16 shows that the total accumulated hours when the heater was turned on to keep the indoor temperature at 20 °C decreased by 119 h after the thermal labyrinth system was installed. Moreover, the heating energy consumption decreased by 8% from 400,754 to 369,413 kWh (Table 11).

Figure 17 shows the indoor and outdoor air temperatures during cooling in August. The set indoor temperature during the cooling season was 26 °C. The indoor temperature exceeded 26 °C immediately before and after the cooling system was turned on whether the thermal labyrinth system was installed or not; however, once the cooling system started operating during the working hours, the indoor temperature remained below 26 °C in both cases. This showed that the cooling system was working normally. The number of hours in which the cooling system operated decreased by 214 when the thermal labyrinth system was installed (Figure 18). Moreover, as the thermal labyrinth system was installed, the cooling energy consumption decreased by 83,266 (from 557,966 to 474,700 kWh), which represented 15% of the total cooling energy consumption. As shown in Table 11, the yearly total air conditioning energy consumption decreased by about 12% from 958,721 to 844,114 kWh.

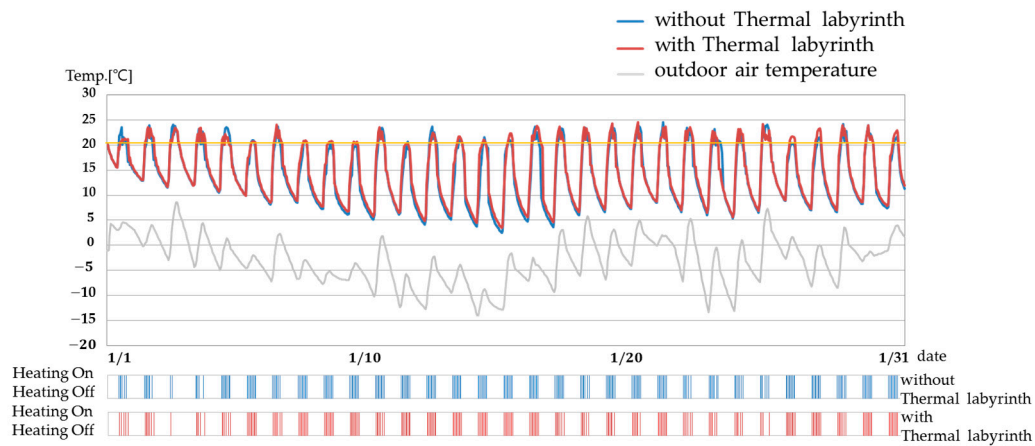


Figure 15. Outdoor and indoor air temperature distributions during heating.

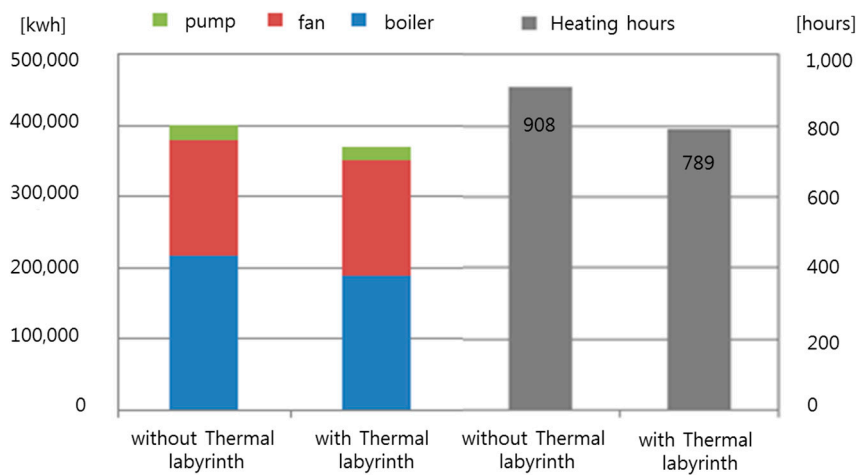


Figure 16. Heating energy consumption and heating hours.

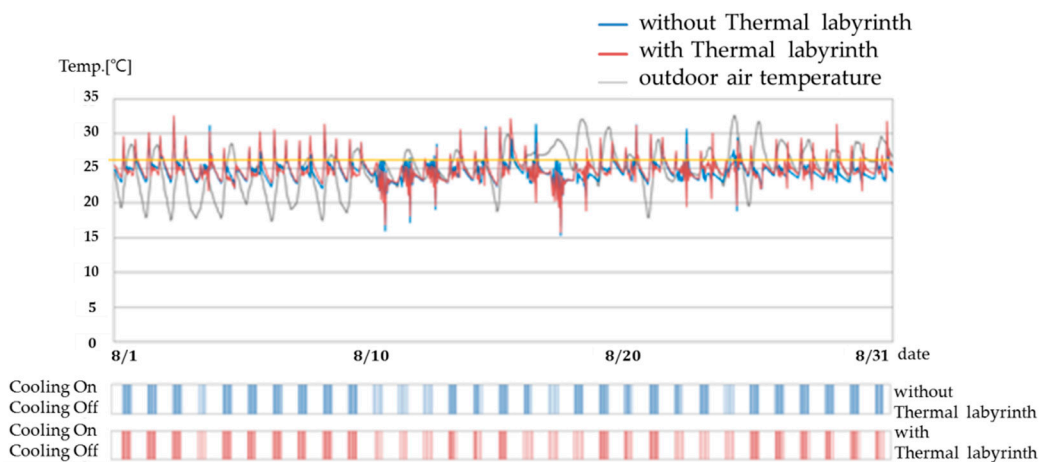


Figure 17. Outdoor and indoor air temperature distributions during cooling.

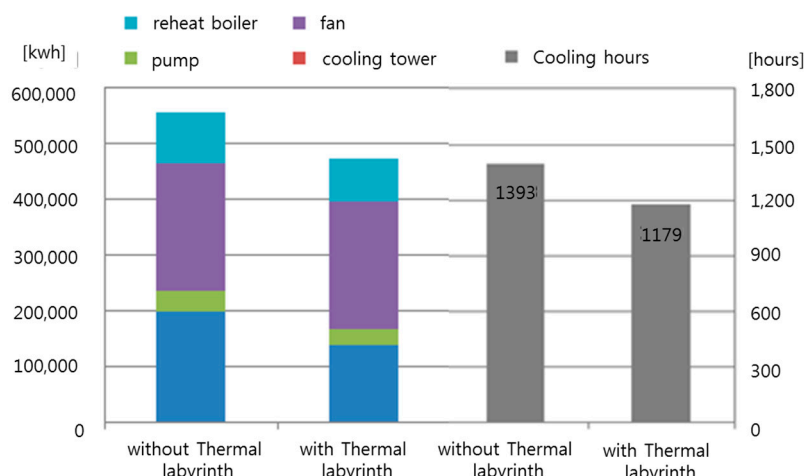


Figure 18. Cooling energy consumption and cooling hours.

Table 11. Energy saving ratio for air conditioning.

Item	Without Thermal Labyrinth	With Thermal Labyrinth	Reduction Rate
Heating energy consumption [kwh]	400,754	369,413	8%
Cooling energy consumption [kwh]	557,966	474,700	15%
Annual total energy consumption [kwh]	958,721	844,114	12%

4.3. Calculation of the Payback Period

The economic feasibility of the optimized thermal labyrinth was analyzed using a simple payback period estimated from the increase in construction costs and saving in annual energy costs. The increased capital costs of the thermal labyrinth was 96,060,000 won, and the reduction cost in the annual energy use was calculated about 9,668,247 won (Table 12). Korea Electric Power Corp. data were used for unit price. Considering the increase in construction cost and the saving in energy cost, the payback period of the optimized thermal labyrinth was determined to be 9.9 years. In previous studies by Song et al. [18] and Paul et al. [19] the payback period of system was 12.1 years and 26 years respectively. This study minimized the increase of construction cost by utilizing basement floor space of existing buildings differently from existing research which required additional construction work. This could reduce the payback period.

Table 12. Reduction in the annual energy costs.

Item	Without Thermal Labyrinth [A]		With Thermal Labyrinth [B]		[A] – [B]	
	Heating	Cooling	Heating	Cooling	Heating	Cooling
Electricity use [kwh]	400,754	557,966	369,413	474,700	31,341	83,266
Electricity cost [Korean won]	33,807,607	47,070,012	31,163,681	40,045,692	2,643,926	7,024,320
Total cost [Korean won]	80,877,619		71,209,373		9,668,247	

5. Conclusions

In this study, a thermal labyrinth system design that can maximize the heat transfer efficiency was developed, and its optimal operation mode was estimated. The results indicated efficient operation conditions for the thermal labyrinth system. The yearly air-conditioning energy-saving effect of the optimized thermal labyrinth system was also analyzed based on the proposed operation mode. The results of this study can be summarized as follows:

- (1) Case studies were conducted to increase the efficiency of the thermal labyrinth system. The results showed that the internal space should be relatively wide. Moreover, embossed internal surfaces should be formed on the walls and floor to achieve an efficient thermal labyrinth system.
- (2) The yearly performance analysis of the optimized thermal labyrinth system showed that the COP was highest in summer (August) and winter (January), when there was a marked difference between the outdoor air temperature and the temperature of the air that passed through the thermal labyrinth. On the other hand, in the transitional period (April or October), the outdoor air temperature was similar to that of the air that passed through the thermal labyrinth; thus, there was no active heat transfer, and the COP was low (below 1.0). Additionally, an equation that expresses the relationship between the outdoor air temperature and the temperature of the air that passed through the thermal labyrinth was proposed.
- (3) A yearly operation algorithm was proposed based on the indoor, outdoor air, thermal labyrinth outlet, and ground temperatures, which resulted in five operation modes. Moreover, in three of the five operation modes, air-conditioning based on the thermal labyrinth system was effective.
- (4) The energy-saving effect from air-conditioning using the optimized thermal labyrinth system on the target building was analyzed under the operation mode. The results showed that in 30% of the air-conditioning load produced by the thermal labyrinth system, the heating and cooling energy consumptions were reduced by 8% and 15%, respectively, which reduced the total air-conditioning energy consumption by about 12%.
- (5) According to the increase in construction cost and the saving in energy cost, the payback period of the optimized thermal labyrinth was determined to be 9.9 years.

The present study suggests methods for improving the efficiency of the pre-heating and pre-cooling systems using ground heat, a clean type of energy, and management plans. It suggests that the heat transfer efficiency can be greatly improved using the proposed system design when implementing a system based on ground heat. Moreover, it shows that the annual system management energy efficiency can only be increased when various methods of operation are applied according to the external environmental conditions. In addition, it suggests a methodology for analyzing these conditions according to fluid analysis simulations and energy analysis simulations. These results are very important to the future HVAC system development and in studies investigating energy efficiency.

Author Contributions: Conceptualization, M.R.; Data curation, M.R.; Formal analysis, M.R.; Funding acquisition, U.-J.S.; Methodology, T.K.; Project administration, T.K.; Resources, T.K.; Software, M.R.; Supervision, T.K.; Writing—original draft, M.R.; Writing—review & editing, M.R. and T.K.

Funding: This work was supported by the Korea Institute of Energy Technology Evaluation and Planning (KETEP) and the Ministry of Trade, Industry & Energy (MOTIE) of the Republic of Korea (No. 20162010104270).

Acknowledgments: This work was supported by the Korea Institute of Energy Technology Evaluation and Planning (KETEP) and the Ministry of Trade, Industry & Energy (MOTIE) of the Republic of Korea (No. 20162010104270).

Conflicts of Interest: The authors declare no conflict of interest.

References

1. Darkwa, J.; Kokogiannakis, G.; Magadzire, C.L.; Yuan, K. Theoretical and Practical Evaluation of an Earth-tube (E-tube) Ventilation System. *Energy Build.* **2011**, *43*, 728–736. [[CrossRef](#)]
2. Al-Ajmi, F.; Loveday, D.L.; Hanby, V.I. The Cooling Potential of Earth-Air-Heat Exchangers for Domestic Buildings in a Desert Climate. *Build. Environ.* **2006**, *41*, 23–24. [[CrossRef](#)]
3. Ghosal, M.K.; Tiwari, G.N. Modeling and Parametric Studies of the Thermal Performance of an Earth-to-Air Heat Exchanger Integrated with a Greenhouse. *Energy Convers. Manag.* **2006**, *47*, 1779–1798. [[CrossRef](#)]
4. Yoon, G.; Masaya, O.; Hideki, T. Study on the Design Procedure for a Multi-cool/heat Tube System. *Sol. Energy* **2009**, *83*, 1415–1424. [[CrossRef](#)]
5. Misra, R.; Das Agrawal, G.; Mathur, J.; Vikas, B.; Aseri, T.K. CFD-analysis-based Parametric Study of the Derating Factor for the Earth Air Tunnel Heat Exchanger. *Energy Build.* **2012**, *49*, 531–535. [[CrossRef](#)]

6. Ascione, F.; Bella, L.; Minichiello, F. Earth-to-air heat exchangers for Italian climates. *Renew. Energy* **2001**, *36*, 2177–2188. [[CrossRef](#)]
7. Ozgener, L. A review on the experimental and analytical analysis of earth to air heat exchanger (EAHE) system in Turkey. *Renew. Sustain. Energy Rev.* **2011**, *15*, 4483–4490. [[CrossRef](#)]
8. Sanusi, A.; Shao, L.; Ibrahim, N. Passive ground cooling system for low energy buildings in Malaysia (hot and humid climates). *Renew. Energy* **2013**, *49*, 193–196. [[CrossRef](#)]
9. Yu, Y.; Li, H.; Niu, F.; Yu, D. Investigation of a coupled geothermal cooling system with earth tube and solar chimney. *Appl. Energy* **2014**, *114*, 209–217. [[CrossRef](#)]
10. Ghosal, M.K.; Tiwari, G.N.; Das, D.K.; Pandey, K.P. Modeling and Comparative Thermal Performance of the Ground Air Collector and the Earth Air Heat Exchanger for the Heating of a Greenhouse. *Energy Build.* **2005**, *37*, 613–621. [[CrossRef](#)]
11. Bansal, V.; Misra, R.; Das Agrawal, G.; Mathur, J. Performance Evaluation and Economic Analysis of the Integrated Earth-Air-Tunnel Heat Exchanger: Evaporative Cooling System. *Energy Build.* **2012**, *55*, 102–108. [[CrossRef](#)]
12. Yang, D.; Zhang, J. Analysis and experiments on the periodically fluctuating air temperature in a building with earth-air tube ventilation. *Build. Environ.* **2015**, *85*, 29–39. [[CrossRef](#)]
13. Song, S.-Y.; Song, J.-H.; Lim, J.-H. An Analysis of the Yearly Energy Performance and Economic Performance of the Thermal Labyrinth Ventilation System. *J. Archit. Inst. Korea* **2012**, *28*, 265–276.
14. Wondeuk, S.; Sung, L. Study on the Fresh Air Load Reduction System Using the Geothermal Energy Effect on the Thermal Characteristic and Air Pattern of the System According to the Opening Configuration. *Korean J. Air-Cond. Refrig. Eng.* **2004**, *16*, 1092–1100.
15. Bansal, V.; Rohit, M.; Das Agarwal, G.; Mathur, J. Transient effect of soil thermal conductivity and duration of operation on performance of Earth Air Tunnel Heat Exchanger. *Appl. Energy* **2013**, *103*, 1–11. [[CrossRef](#)]
16. Krati, M.; Lopez-Alonzo, C.; Claridge, D.E.; Kreider, J.F. Analysis Model to Predict Non-homogeneous Soil Temperature Variation. *J. Sol. Energy Eng.* **1995**, *117*, 100–107. [[CrossRef](#)]
17. Cho, J. Thermal Analysis of Outer Walls Adjoining the Underground for the Use of Underground Spaces. Master's Thesis, Yonsei University, Seoul, Korea, 2001.
18. Song, S.-Y.; Song, J.-H.; Lim, J.-H. Effectiveness of a thermal labyrinth ventilation system using geothermal energy: A case study of an educational facility in South Korea. *Energy Sustain. Dev.* **2014**, *23*, 150–164. [[CrossRef](#)]
19. Paul, M.; Ray, P. Large Dynamic Thermal Labyrinth: A Step Towards Net Zero Energy Use in Acute Care Hospitals. In Proceedings of the 2012 ACEEE Summer Study on Energy Efficiency in Buildings, Pacific Grove, CA, USA, 12 August 2012; American Council for an Energy-Efficient Economy: Washington, DC, USA, 2012.

